SIAM J. IMAGING SCIENCES
Vol. 2, No. 2, pp. 646–669

On the Use of Start-Stop Approximation for Spaceborne SAR Imaging*

S. V. Tsynkov†

Abstract. The start-stop approximation is a standard tool for processing radar data in synthetic aperture imaging. It assumes that the antenna is motionless when a pulse is emitted and the scattered signal received, after which the antenna moves to its next sending/receiving position along the flight track. However, when the antenna is mounted on a satellite, as opposed to an airplane, its relatively high speed raises at least two questions. The first one is whether the image may be affected by the actual displacement of the antenna during the pulse round-trip time between the orbit and the Earth's surface. This displacement, in fact, can be rather large. Nonetheless, by analyzing the corresponding generalized ambiguity function of a synthetic aperture radar (SAR) sensor we show that in practice this issue can be disregarded. The second question is related to the Doppler frequency shift, which, again, is larger for spaceborne radars than for airborne radars. In the early SAR studies, this frequency shift provided a venue for understanding the azimuthal resolution of a radar. However, in a more rigorous analysis based on the generalized ambiguity function, the Doppler effect is typically left out of consideration. We show that for the image to stay largely unaffected by Doppler, the frequency shift must be included in the definition of a matched filter. Otherwise, there will be a geometric shift (translation) of the entire imaged scene from its true position, and there may also be a slight deterioration of the image sharpness (contrast).

Key words. synthetic aperture radar (SAR), spaceborne SAR imaging, high-speed motion, start-stop approximation, Doppler effect, Lorentz transform, displacement of the antenna, range and azimuthal resolution, image sharpness (contrast)

AMS subject classifications. 78A40, 78A45, 78A46, 78A50, 78A55, 78M35, 78M99

DOI. 10.1137/08074026X

1. Introduction.

A synthetic aperture radar (SAR) builds an image of a target (which could be an area of the Earth's surface) by successively illuminating it with a series of electromagnetic pulses transmitted from different locations and subsequently processing the scattered waves with the help of a matched filter. Typically, the antenna of such a radar is mounted on an aircraft (airborne radar) or a satellite (spaceborne radar), and the interrogating pulses are emitted and received as the craft travels along its flight track or orbit, respectively. A standard approach employed when processing the SAR data is based on the start-stop approximation, when the antenna is assumed to be at a standstill while it sends a pulse and receives the scattered response, after which it moves on to the position where the next pulse is emitted; see, e.g., [3, 7, 8] and also [4]. This approximation is intuitively well justified for an airborne radar. Indeed, a typical aircraft speed is between 200m/sec and 300m/sec. Then, even when the look angle is large (close to $\pi/2$) so that the radar scans the surface far to the

*Received by the editors November 10, 2008; accepted for publication (in revised form) February 13, 2009; published electronically May 14, 2009. This work was supported by the U.S. Air Force Office of Scientific Research (AFOSR) under grant FA9550-07-1-0170.
http://www.siam.org/journals/siims/2-2/74026.html
†Department of Mathematics, North Carolina State University, Box 8205, Raleigh, NC 27695 (tsynkov@math.ncsu.edu, http://www.math.ncsu.edu/~stsynkov).

side rather than directly underneath the flight track, the round-trip travel time for the pulse will still be under 10^{-3}sec. This yields the displacement of the antenna between 20cm and 30cm (see section 3), which is on the order of one to a few wavelengths for the microwave frequency band that the radar typically operates in and is also far shorter than the typical antenna size. Besides, the magnitude of the linear Doppler frequency shift in this case is rather small—under 10^{-6}; see section 4.

On the other hand, using the start-stop approximation for a spaceborne radar may raise questions. With the round-trip travel times $\sim 1/200$sec and the speed of 8km/sec, the displacement of the antenna over the period of time between the emission and arrival of a pulse may reach about 40m, which is several times longer than the antenna size and much larger than the wavelength. It is not clear ahead of time whether neglecting this displacement may affect the quality of the image. Moreover, the Doppler frequency shift, which is $\sim v/c$, where v is the speed of the satellite and c is the speed of light (see section 4), will also be about one and a half orders of magnitude larger than in the case of an airborne radar. In the earlier SAR studies, the Doppler shift was used to explain the mechanism of along-the-track resolution; see, e.g., [8]. However, when building a generalized ambiguity function the Doppler effect is often neglected, and it is not apparent whether it may cause a deterioration of the image.

In this paper we analyze the generalized ambiguity function of a SAR system (see section 2) while taking the two foregoing phenomena into account. Our analysis shows that the displacement of the antenna, even though quite noticeable, has a very small detrimental effect $\mathcal{O}(v/c)$ on the resolution of the image and can therefore be disregarded for all practical purposes; see section 3. As for the Doppler effect, disregarding it in the generalized ambiguity function may cause an overall translation of the entire scene on the image, as well as a slight deterioration of the sharpness (contrast); see section 4. To avoid this, one must include the frequency shift into the definition of a matched filter.

2. Generalized ambiguity function. For the analysis in the paper, we will employ the following assumptions. The electromagnetic field propagating between the antenna and the target will be assumed scalar and will be governed by the standard d'Alembert equation with the speed c (the speed of light). In other words, we will disregard the polarization. The image will be assumed two-dimensional; i.e., the radar will measure coordinates of the targets along the Earth's surface but will not measure their elevation. All targets will be assumed dispersionless, and scattering off the targets will be linearized and analyzed using the first Born approximation; see [2, section 13.1.4].

The radar will be assumed to operate in the standard mode known as stripmap; see [3]. In this case, the antenna points in the direction which is fixed relative to that of the satellite motion. Hence, the footprint of the beam emitted by the antenna sweeps a strip on the Earth's surface parallel to flight track, i.e., to the orbit. In doing so, the antenna does not necessarily have to point precisely sideways, i.e., normally to the direction of motion. Instead, it can point either forward or backward at a fixed angle, which corresponds to the so-called squinted stripmap mode.

Finally, we will need to use the Lorentz transform [9, Chapter 3, section 3] that preserves the form of the d'Alembert equation in the case of moving transmitters and/or receivers; see section 4. To be able to do so, we will have to assume that the motion of the antenna is straightforward and uniform. Technically speaking, this is not true for a satellite orbiting the

Earth. However, for a relatively short stretch of the orbit, along which the measurements are taken of a given small target (i.e., for which a given target stays in the beam; see section 3), this is a sufficiently accurate approximation.

Hereafter, we adopt some notation of [4]. The interrogating pulses emitted by the antenna of a SAR are taken as linear upchirps of the form

$$P(t) = A(t)e^{i\omega_0 t}, \quad \text{where} \quad A(t) = \chi_\tau(t)e^{i\alpha t^2}. \tag{2.1}$$

In formula (2.1), $\chi_\tau(t)$ is the indicator function of the interval of duration τ,

$$\chi_\tau(t) = \begin{cases} 1, & t \in [-\tau/2, \tau/2], \\ 0 & \text{otherwise}, \end{cases}$$

and $\alpha = B/(2\tau)$, where B is the bandwidth of the chirp. Accordingly, the instantaneous frequency of the chirp is given by

$$\omega(t) = \omega_0 + \frac{Bt}{\tau}, \quad t \in [-\tau/2, \tau/2], \tag{2.2}$$

where ω_0 is the center carrier frequency. The modulating function $A(t)$ in formula (2.1) is assumed to be slowly varying compared to the fast carrier oscillation $e^{i\omega_0 t}$.

Suppose first that the antenna is a motionless point source located at $\boldsymbol{x} \in \mathbb{R}^3$. Then, the propagating field due to the emitted chirp (2.1) is given by the standard retarded potential:

$$\varphi(t, \boldsymbol{z}) = \frac{1}{4\pi} \frac{P(t - |\boldsymbol{z} - \boldsymbol{x}|/c)}{|\boldsymbol{z} - \boldsymbol{x}|}. \tag{2.3}$$

Let us assume that the imaged terrain, which is also motionless, is characterized by the variable refraction index $n = n(\boldsymbol{z})$. Under the first Born approximation [2, section 13.1.4], scattering is linearized so that the terrain is interpreted as a secondary wave's source due to the incident field $\varphi(t, \boldsymbol{z})$ of (2.3):

$$\frac{1 - n^2(\boldsymbol{z})}{c^2} \frac{\partial^2 \varphi}{\partial t^2} \stackrel{\text{def}}{=} \nu(\boldsymbol{z}) \frac{\partial^2 \varphi}{\partial t^2}.$$

Consequently, the scattered field at the location $\tilde{\boldsymbol{x}}$ and time t is given by the Kirchhoff integral:

$$\psi(t, \tilde{\boldsymbol{x}}) = \frac{1}{4\pi} \iiint_{|\tilde{\boldsymbol{x}} - \boldsymbol{z}| \le ct} \frac{\nu(\boldsymbol{z})}{|\tilde{\boldsymbol{x}} - \boldsymbol{z}|} \frac{\partial^2 \varphi}{\partial t^2} (t - |\tilde{\boldsymbol{x}} - \boldsymbol{z}|/c, \boldsymbol{z})\, d\boldsymbol{z}. \tag{2.4}$$

As the amplitude $A(t)$ in (2.1) is slowly varying, it can be left out when differentiating the incident field (2.3) for substitution into (2.4), which yields

$$\frac{\partial^2 \varphi}{\partial t^2}(t, \boldsymbol{z}) \approx -\frac{\omega_0^2}{4\pi} \frac{P(t - |\boldsymbol{z} - \boldsymbol{x}|/c)}{|\boldsymbol{z} - \boldsymbol{x}|}. \tag{2.5}$$

Consequently,

$$\begin{aligned} \psi(t, \tilde{\boldsymbol{x}}) &\approx -\frac{\omega_0^2}{16\pi^2} \iiint_{|\tilde{\boldsymbol{x}} - \boldsymbol{z}| \le ct} \frac{\nu(\boldsymbol{z})}{|\tilde{\boldsymbol{x}} - \boldsymbol{z}||\boldsymbol{z} - \boldsymbol{x}|} P\left(t - |\tilde{\boldsymbol{x}} - \boldsymbol{z}|/c - |\boldsymbol{z} - \boldsymbol{x}|/c\right) d\boldsymbol{z} \\ &= -\frac{\omega_0^2}{16\pi^2} \iiint_{|\tilde{\boldsymbol{x}} - \boldsymbol{z}| \le ct} \frac{\nu(\boldsymbol{z})}{|\tilde{\boldsymbol{x}} - \boldsymbol{z}||\boldsymbol{z} - \boldsymbol{x}|} A\left(t - |\tilde{\boldsymbol{x}} - \boldsymbol{z}|/c - |\boldsymbol{z} - \boldsymbol{x}|/c\right) e^{i\omega_0 (t - |\tilde{\boldsymbol{x}} - \boldsymbol{z}|/c - |\boldsymbol{z} - \boldsymbol{x}|/c)} d\boldsymbol{z}. \end{aligned} \tag{2.6}$$

Formula (2.6) indicates that the scattered field $\psi(t,\tilde{\boldsymbol{x}})$ is obtained by applying a Fourier integral operator to the target reflectivity function $\nu(\boldsymbol{z})$; see, e.g., [5, 6]. The key goal of radar imaging is to build an (approximate) inverse to this operator and thus reconstruct $\nu(\boldsymbol{z})$ from the observed scattered field.

We perform the approximate inversion in two stages; first, we apply a matched filter to the field ψ, and then we accumulate the information due to multiple interrogating pulses (2.1) emitted from and received at different locations on the orbit. As one will see from our subsequent analysis (a more detailed derivation can be found in [4, 5, 6]), this procedure resembles the application of an adjoint operator, which would have coincided with the true inverse if the mapping (2.6) was a standard Fourier transform (a unitary operator).

The matched filter is defined as follows. Assume that there is a point scatterer at a reference location $\boldsymbol{y}$; then the resulting field at $(t,\tilde{\boldsymbol{x}})$ is obtained by substituting $\nu(\boldsymbol{z})=\delta(\boldsymbol{z}-\boldsymbol{y})$ into formula (2.6):

$$\psi_1(t,\tilde{\boldsymbol{x}}) = -\frac{\omega_0^2}{16\pi^2}\frac{P(t-|\tilde{\boldsymbol{x}}-\boldsymbol{y}|/c-|\boldsymbol{y}-\boldsymbol{x}|/c)}{|\tilde{\boldsymbol{x}}-\boldsymbol{y}||\boldsymbol{y}-\boldsymbol{x}|}. \tag{2.7}$$

The filter is essentially a complex conjugate of ψ_1 given by (2.7); for simplicity, the constant factor $-\omega_0^2/16\pi^2$ and the entire denominator, which is a slowly varying function (compared to the fast oscillation $e^{i\omega_0 t}$), are disregarded. What remains is merely $\overline{P(t-|\tilde{\boldsymbol{x}}-\boldsymbol{y}|/c-|\boldsymbol{y}-\boldsymbol{x}|/c)}$, where the overbar denotes complex conjugation. The application of this filter yields the image:

$$\begin{aligned} I(\boldsymbol{y}) &= \int \overline{P(t-|\tilde{\boldsymbol{x}}-\boldsymbol{y}|/c-|\boldsymbol{y}-\boldsymbol{x}|/c)}\psi(t,\tilde{\boldsymbol{x}})dt \\ &= -\frac{\omega_0^2}{16\pi^2}\iiint_{|\tilde{\boldsymbol{x}}-\boldsymbol{z}|\le ct} \underbrace{\int \overline{P(t-|\tilde{\boldsymbol{x}}-\boldsymbol{y}|/c-|\boldsymbol{y}-\boldsymbol{x}|/c)}P(t-|\tilde{\boldsymbol{x}}-\boldsymbol{z}|/c-|\boldsymbol{z}-\boldsymbol{x}|/c)dt}_{W(\boldsymbol{y},\boldsymbol{z})} \\ &\qquad \cdot \frac{\nu(\boldsymbol{z})}{|\tilde{\boldsymbol{x}}-\boldsymbol{z}||\boldsymbol{z}-\boldsymbol{x}|}d\boldsymbol{z}, \end{aligned} \tag{2.8}$$

where we have changed the order of integration after substituting expression (2.6) for $\psi(t,\tilde{\boldsymbol{x}})$. The interior integral that we denote $W(\boldsymbol{y},\boldsymbol{z})$ in formula (2.8) is called the point spread function[1]; see [4]. Up to a slowly varying denominator, the point spread function $W(\boldsymbol{y},\boldsymbol{z})$ yields the image of a point scatterer located at $\boldsymbol{z}$; i.e., it is the field due to a unit magnitude delta-function at $\boldsymbol{z}$ processed with the matched filter $\overline{P(\,\cdot\,)}$.

The antenna of a real SAR sensor emits and receives a series of chirps (2.1) as the satellite travels along the orbit. Let us therefore consider a sequence of emitting times and locations $(t_n,\boldsymbol{x}^n)$ and the corresponding sequence of receiving locations $\tilde{\boldsymbol{x}}^n$. For each n, we build the point spread function following (2.8):

$$W_n(\boldsymbol{y},\boldsymbol{z}) = \int \overline{P(t-t_n-|\tilde{\boldsymbol{x}}^n-\boldsymbol{y}|/c-|\boldsymbol{y}-\boldsymbol{x}^n|/c)}P(t-t_n-|\tilde{\boldsymbol{x}}^n-\boldsymbol{z}|/c-|\boldsymbol{z}-\boldsymbol{x}^n|/c)dt. \tag{2.9}$$

[1]Recall that both $I(\boldsymbol{y})$ and $W(\boldsymbol{y},\boldsymbol{z})$ also depend on the emitting and receiving locations $\boldsymbol{x}$ and $\tilde{\boldsymbol{x}}$, respectively.

The generalized ambiguity function of a SAR system takes into account the information from multiple interrogating pulses by summing up the corresponding contributions (2.9):

$$W(\boldsymbol{y},\boldsymbol{z}) = \sum_n \vartheta(\boldsymbol{z},\boldsymbol{x}^n) W_n(\boldsymbol{y},\boldsymbol{z}). \tag{2.10}$$

The factor $\vartheta(\boldsymbol{z},\boldsymbol{x}^n)$ under the sum in (2.10) determines the range of summation. It comes from the directivity pattern of the antenna, because in real-life settings the antenna is never a point monopole with isotropic radiation. In fact, the actual antenna emits a rather narrow beam (see [4]), and the quantity $\vartheta(\boldsymbol{z},\boldsymbol{x}^n)$ can be approximated as follows:

$$\vartheta(\boldsymbol{z},\boldsymbol{x}^n) = \begin{cases} 1 & \text{if the target } \boldsymbol{z} \text{ is in the beam emitted from } \boldsymbol{x}^n, \\ 0 & \text{otherwise.} \end{cases}$$

We will see later (in section 3) how to determine whether a given target is in the antenna beam or not. We will also see that it is precisely the summation (2.10) that can help interpret the processing of the received field $\psi(t,\tilde{\boldsymbol{x}})$ in the sense of the (discrete) inverse Fourier transform (sections 3 and 4).

The generalized ambiguity function (2.10) is a key construct that allows one to analyze the performance of a SAR system. Indeed, it yields the image of an ultimately simplified target, which is a point scatterer, whereas other, more complex, targets can be assembled using point scatterers (in the usual way, as convolution with the Dirack delta-function). Of central importance in terms of performance is the resolution of a radar, i.e., its ability to distinguish between two different targets located at a certain distance apart. If we could make the generalized ambiguity function (2.10) equal to the delta-function, $W(\boldsymbol{y},\boldsymbol{z}) = \delta(\boldsymbol{y}-\boldsymbol{z})$, then the radar would have an ideal resolution. In reality, however, this is never achieved, but the sharper (i.e., narrower) the peak that $W(\boldsymbol{y},\boldsymbol{z})$ has when the reference location $\boldsymbol{y}$ approaches the actual target location $\boldsymbol{z}$, the better.

Note that in most studies of monostatic SAR resolution,[2] the receiving locations $\tilde{\boldsymbol{x}}^n$ are taken to be the same as the emitting locations $\boldsymbol{x}^n$. This corresponds to the start-stop approximation, when the antenna emits the interrogating pulse and receives the scattered response while at the same position, and then continues to move along the orbit to the next position. We, on the other hand, have intentionally allowed for the receiving and emitting locations to differ in the expressions for the point spread function (2.9) and the generalized ambiguity function (2.10). This will let us take into account the actual antenna displacement during the pulse round-trip time between the orbit and the ground and thus analyze the effect of the start-stop approximation on the quality of the image; see section 3. Note also that formulae (2.9) and (2.10) assume that both the antenna and the target are motionless when the pulse is emitted and received. To account for the motion and hence for the Doppler effect, the expressions for the point spread function and the generalized ambiguity function will be modified with the help of the Lorentz transform; see section 4.

[2]Bistatic systems, unlike monostatic systems, have separately located transmitting and receiving antennas; see, e.g., [3, p. 18].

3. Antenna displacement. For the analysis of SAR resolution, the generalized ambiguity function (2.10) can be conveniently decomposed into the product of two factors, transverse and longitudinal, that will be responsible for the range and azimuthal (i.e., cross-range) resolution, respectively; see [4]. To do so, we first use formulae (2.1) and (2.9) and recast expression (2.10) as follows:

$$W(\boldsymbol{y},\boldsymbol{z}) = \sum_n \vartheta(\boldsymbol{z},\boldsymbol{x}^n) \int \overline{A(t-t_n-|\tilde{\boldsymbol{x}}^n-\boldsymbol{y}|/c-|\boldsymbol{y}-\boldsymbol{x}^n|/c)} e^{i\omega_0(|\tilde{\boldsymbol{x}}^n-\boldsymbol{y}|/c+|\boldsymbol{y}-\boldsymbol{x}^n|/c)} \times A(t-t_n-|\tilde{\boldsymbol{x}}^n-\boldsymbol{z}|/c-|\boldsymbol{z}-\boldsymbol{x}^n|/c) e^{-i\omega_0(|\tilde{\boldsymbol{x}}^n-\boldsymbol{z}|/c+|\boldsymbol{z}-\boldsymbol{x}^n|/c)} dt. \tag{3.1}$$

Next, we take the new integration variable as $t-t_n$ in each term of the sum (3.1) and denote it by t again. Then, we realize that neither $\overline{A(t-|\tilde{\boldsymbol{x}}^n-\boldsymbol{y}|/c-|\boldsymbol{y}-\boldsymbol{x}^n|/c)}$ nor $A(t-|\tilde{\boldsymbol{x}}^n-\boldsymbol{z}|/c-|\boldsymbol{z}-\boldsymbol{x}^n|/c)$ depends on n explicitly, except for the dependence via $\boldsymbol{x}^n$ and $\tilde{\boldsymbol{x}}^n$. The latter is weak, because we are assuming that the distance from the orbit to the ground is much larger than the distance between the successive emitting (or receiving) positions of the antenna on the orbit. Hence, $|\boldsymbol{y}-\boldsymbol{x}^n|/c$, etc., are slowly varying functions of n, and on top of it we have another slowly varying function $A(\cdot)$. Therefore, the amplitudes $A(\cdot)$ and $\overline{A(\cdot)}$ can be taken outside the sum (3.1), and we obtain

$$W(\boldsymbol{y},\boldsymbol{z}) \approx \underbrace{\Big(\sum_n \vartheta(\boldsymbol{z},\boldsymbol{x}^n) e^{i\omega_0(|\tilde{\boldsymbol{x}}^n-\boldsymbol{y}|/c+|\boldsymbol{y}-\boldsymbol{x}^n|/c-|\tilde{\boldsymbol{x}}^n-\boldsymbol{z}|/c-|\boldsymbol{z}-\boldsymbol{x}^n|)}\Big)}_{W_A(\boldsymbol{y},\boldsymbol{z})} \times \underbrace{\Big(\int \overline{A(t-|\tilde{\boldsymbol{x}}^0-\boldsymbol{y}|/c-|\boldsymbol{y}-\boldsymbol{x}^0|/c)} A(t-|\tilde{\boldsymbol{x}}^0-\boldsymbol{z}|/c-|\boldsymbol{z}-\boldsymbol{x}^0|/c)dt\Big)}_{W_R(\boldsymbol{y},\boldsymbol{z})},$$

where we have replaced the superscript "n" by "0" in the factor $W_R(\boldsymbol{y},\boldsymbol{z})$ for definiteness. Consequently, the generalized ambiguity function can be (approximately) represented as a product of the azimuthal factor,

$$W_A(\boldsymbol{y},\boldsymbol{z}) = \sum_n \vartheta(\boldsymbol{z},\boldsymbol{x}^n) e^{i\omega_0(|\tilde{\boldsymbol{x}}^n-\boldsymbol{y}|/c+|\boldsymbol{y}-\boldsymbol{x}^n|/c-|\tilde{\boldsymbol{x}}^n-\boldsymbol{z}|/c-|\boldsymbol{z}-\boldsymbol{x}^n|/c)}, \tag{3.2}$$

and the range factor,

$$W_R(\boldsymbol{y},\boldsymbol{z}) = \int \overline{A(t-|\tilde{\boldsymbol{x}}^0-\boldsymbol{y}|/c-|\boldsymbol{y}-\boldsymbol{x}^0|/c)} A(t-|\tilde{\boldsymbol{x}}^0-\boldsymbol{z}|/c-|\boldsymbol{z}-\boldsymbol{x}^0|/c)dt. \tag{3.3}$$

We will see that the factor $W_A(\boldsymbol{y},\boldsymbol{z})$ of (3.2) is responsible for the resolution in the longitudinal, or azimuthal, direction (i.e., along the orbit), whereas the factor $W_R(\boldsymbol{y},\boldsymbol{z})$ of (3.3) is responsible for the resolution in the transverse, or range, direction (perpendicular to the orbit).

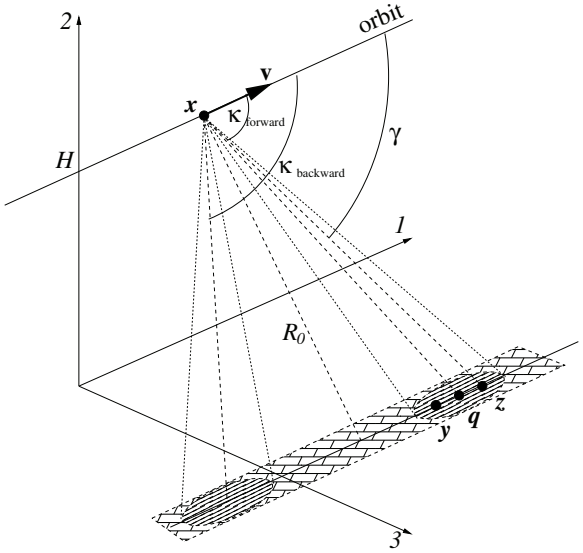

Figure 1. *SAR imaging schematic for the squinted stripmap mode with the antenna pointing either forward or backward:* $\kappa_{\text{forward}} < \pi/2$ *and* $\kappa_{\text{backward}} > \pi/2$.

3.1. Azimuthal resolution. Hereafter, we will denote individual Cartesian coordinates by subscripts: $\boldsymbol{x} = (x_1, x_2, x_3)$, $\boldsymbol{y} = (y_1, y_2, y_3)$, $\boldsymbol{z} = (z_1, z_2, z_3)$. With no loss of generality we can assume that the orbit is parallel to the Cartesian direction "1" (recall that we are considering only short stretches of the orbit and hence can neglect its curvature). To analyze the azimuthal resolution we will assume that both the target $\boldsymbol{z}$ and the reference point $\boldsymbol{y}$ are located on the Earth's surface at the same distance R_0 from the orbit; see Figure 1. Let κ denote the angle between the velocity $\boldsymbol{v}$ of the satellite (positive x_1 direction) and the direction of the antenna beam (i.e., its central line). If $\kappa < \pi/2$, then the antenna is pointing forward; if $\kappa > \pi/2$, then the antenna is pointing backward; and the value $\kappa = \pi/2$ corresponds to broadside imaging.

Let us denote the center of the antenna beam footprint on the Earth's surface by $\boldsymbol{q} = (q_1, q_2, q_3)$. Clearly, we have $q_1 = x_1 + R_0 \cot\kappa$; see Figure 1. Hereafter, we will assume with no loss of generality that both the target $\boldsymbol{z}$ and the reference point $\boldsymbol{y}$ are close to the center of the footprint $\boldsymbol{q}$ so that $|q_1 - z_1| \ll R_0$ and $|q_1 - y_1| \ll R_0$. Then, we can use the law of cosines and the first order Taylor expansion of the square root to obtain approximate expressions for the distances that appear in the exponent in formula (3.2); see Figure 1. For example, we have

$$
\begin{aligned}
|\boldsymbol{z} - \boldsymbol{x}^n| &= \sqrt{\frac{R_0^2}{\sin^2\kappa} + (z_1 - q_1^n)^2 - 2\frac{R_0}{\sin\kappa}(z_1 - q_1^n)\cos(\pi - \kappa)} \\
&= \frac{R_0}{\sin\kappa}\sqrt{1 + \frac{(z_1 - q_1^n)^2 \sin^2\kappa}{R_0^2} + 2\frac{(z_1 - q_1^n)\sin\kappa\cos\kappa}{R_0}} \\
&\approx \frac{R_0}{\sin\kappa} + \frac{(z_1 - q_1^n)^2 \sin\kappa}{2R_0} + (z_1 - q_1^n)\cos\kappa,
\end{aligned}
\tag{3.4}
$$

and, similarly, for the remaining three quantities, $|\boldsymbol{y} - \boldsymbol{x}^n|$, $|\tilde{\boldsymbol{x}}^n - \boldsymbol{y}|$, and $|\tilde{\boldsymbol{x}}^n - \boldsymbol{z}|$.

Expression (3.4) and analogous expressions for other distances need to be substituted into formula (3.2). Before doing that, let us determine the range of summation in (3.2). Let L be the size of the antenna in the direction parallel to the orbit, and let $\lambda = 2\pi c/\omega_0$ denote the carrier wavelength. Typically we have $\lambda \ll L$, in which case the antenna emits a narrow beam with the angular width of approximately $2\lambda/L$; see [4] and [15, Appendix B]. Then, it is easy to see (from Figure 1) that the target $\boldsymbol{z}$ is in the beam as long as

$$|z_1 - q_1^n| \le \frac{R_0}{\sin\kappa}\left(\tan\frac{\lambda}{L}\right)\frac{1}{\sin\kappa} \approx \frac{R_0}{\sin^2\kappa}\frac{\lambda}{L}.$$

Consequently, we can write

$$\vartheta(\boldsymbol{z}, \boldsymbol{x}^n) = \begin{cases} 1 & \text{if } z_1 - \frac{\lambda R_0}{L\sin^2\kappa} \le q_1^n \le z_1 + \frac{\lambda R_0}{L\sin^2\kappa}, \\ 0 & \text{if } q_1^n < z_1 - \frac{\lambda R_0}{L\sin^2\kappa} \text{ or } q_1^n > z_1 + \frac{\lambda R_0}{L\sin^2\kappa}. \end{cases} \tag{3.5}$$

Let Δx_1 be the distance along the orbit between the successive emissions of pulses so that $x_1^n = n\Delta x_1$. Let us also recall that $q_1^n = x_1^n + R_0\cot\kappa$ (see Figure 1) and introduce

$$N = \left[\frac{2\lambda R_0}{\Delta x_1 L\sin^2\kappa}\right] \quad \text{and} \quad N_0 = \left[\frac{z_1 - R_0\cot\kappa}{\Delta x_1}\right],$$

where $[\,\cdot\,]$ stands for the integer part. Then, according to (3.5), we can rewrite the sum (3.2) as follows:

$$W_A(\boldsymbol{y}, \boldsymbol{z}) = \sum_{n=N_0-N/2}^{N_0+N/2} e^{i\omega_0(|\tilde{\boldsymbol{x}}^n - \boldsymbol{y}|/c + |\boldsymbol{y}-\boldsymbol{x}^n|/c - |\tilde{\boldsymbol{x}}^n - \boldsymbol{z}|/c - |\boldsymbol{z}-\boldsymbol{x}^n|/c)}. \tag{3.6}$$

Next, we substitute expression (3.4) and the like into the exponents in formula (3.6). In doing so, we take the terms that do not depend on n outside the sum:

(3.7)

$$\begin{aligned} W_A(\boldsymbol{y}, \boldsymbol{z}) &= e^{\frac{i\omega_0\cos\kappa}{c}(2y_1 - 2z_1)} \sum_{n=N_0-N/2}^{N_0+N/2} e^{\frac{i\omega_0\sin\kappa}{2R_0c}((y_1-\tilde{q}_1^n)^2 + (y_1-q_1^n)^2 - (z_1-\tilde{q}_1^n)^2 - (z_1-q_1^n)^2)} \\ &= e^{\frac{i\omega_0\cos\kappa}{c}(2y_1-2z_1)} e^{\frac{i\omega_0\sin\kappa}{2R_0c}(2y_1^2-2z_1^2)} \sum_{n=N_0-N/2}^{N_0+N/2} e^{\frac{i\omega_0\sin\kappa}{R_0c}(z_1\tilde{q}_1^n + z_1 q_1^n - y_1\tilde{q}_1^n - y_1 q_1^n)} \\ &= e^{\frac{i\omega_0\cos\kappa}{c}(2y_1-2z_1)} e^{\frac{i\omega_0\sin\kappa}{2R_0c}(2y_1^2-2z_1^2)} \sum_{n=N_0-N/2}^{N_0+N/2} e^{\frac{i\omega_0\sin\kappa}{R_0c}(2(z_1-y_1)q_1^n + (z_1-y_1)(\tilde{q}_1^n - q_1^n))}. \end{aligned}$$

We have now arrived at the point when we need to identify a relationship between the quantities q_1^n and $\tilde{q}_1^n$ or, equivalently, between $x_1 = q_1 - R_0\cot\kappa$ and $\tilde{x}_1 = \tilde{q}_1 - R_0\cot\kappa$. For each n, x_1^n denotes the first coordinate of the location at which the nth pulse is emitted, whereas $\tilde{x}_1^n$ is the first coordinate of the location at which the scattered signal is received. Clearly,

$\tilde{q}_1^n - q_1^n = \tilde{x}_1^n - x_1^n = vT$, where $v = |\boldsymbol{v}|$ is the speed of the satellite and $T = T(\boldsymbol{z})$ is the round-trip travel time between the antenna and the target. To find T, let us denote by γ the angle between the velocity $\boldsymbol{v}$ and the direction $\boldsymbol{z} - \boldsymbol{x}$ from the antenna $\boldsymbol{x}$ to the target $\boldsymbol{z}$; it is easy to see from Figure 1 that $\cot\gamma = (z_1 - x_1)/R_0$. Using the law of cosines, we can then write

$$
\begin{aligned}
T(\boldsymbol{z}) &= \frac{|\boldsymbol{z}-\boldsymbol{x}|}{c} + \frac{1}{c}\sqrt{|\boldsymbol{z}-\boldsymbol{x}|^2 + (vT)^2 - 2|\boldsymbol{z}-\boldsymbol{x}|(vT)\cos\gamma} \\
&= \frac{|\boldsymbol{z}-\boldsymbol{x}|}{c} + \frac{1}{c}\sqrt{|\boldsymbol{z}-\boldsymbol{x}|^2 + (vT)^2 - 2(z_1-x_1)(vT)}.
\end{aligned} \tag{3.8}
$$

This is a quadratic equation with respect to T. Solving it, we obtain

$$
T(\boldsymbol{z}) = 2\frac{|\boldsymbol{z}-\boldsymbol{x}|/c - (z_1-x_1)/c(v/c)}{1 - v^2/c^2}. \tag{3.9}
$$

Then, combining (3.9) with (3.4) and disregarding the v^2/c^2 term in the denominator, we can write

$$
\tilde{q}_1^n - q_1^n = vT = 2\frac{v}{c}\cdot\frac{R_0}{\sin\kappa} + \frac{v}{c}\cdot\frac{(z_1-q_1^n)^2\sin\kappa}{R_0} + 2\frac{v}{c}(z_1-q_1^n)\cos\kappa - 2\frac{v^2}{c^2}(z_1-x_1^n). \tag{3.10}
$$

In the previous expression, we can also drop the second term on the right-hand side as it is much smaller than the third term. Consequently, we can continue equality (3.7) as

$$
\begin{aligned}
W_A(\boldsymbol{y},\boldsymbol{z}) &= e^{\frac{i\omega_0\cos\kappa}{c}(2y_1-2z_1)} e^{\frac{i\omega_0\sin\kappa}{2R_0c}(2y_1^2-2z_1^2)} \sum_{n=N_0-N/2}^{N_0+N/2} e^{\frac{i\omega_0\sin\kappa}{R_0c}(z_1-y_1)(2q_1^n+vT)} \\
&= e^{\frac{i\omega_0\cos\kappa}{c}(2y_1-2z_1)} e^{\frac{i\omega_0\sin\kappa}{2R_0c}(2y_1^2-2z_1^2+2(z_1-y_1)\frac{v}{c}(\frac{R_0}{\sin\kappa}+z_1\cos\kappa))} \sum_{n=N_0-N/2}^{N_0+N/2} e^{\frac{i\omega_0\sin\kappa}{R_0c}2(z_1-y_1)(1-\frac{v}{c}\cos\kappa)q_1^n},
\end{aligned}
$$

where we have taken the factors that do not depend on n outside the sum, and, additionally, we have neglected the last term of (3.10) in the exponent as it was only a $\sim v^2/c^2$ correction to the zeroth order term. Then,

$$
\begin{aligned}
W_A(\boldsymbol{y},\boldsymbol{z}) &= e^{\frac{i\omega_0\cos\kappa}{c}(2y_1-2z_1)} e^{\frac{i\omega_0\sin\kappa}{R_0c}(y_1^2-z_1^2+(z_1-y_1)(\frac{v}{c}(\frac{R_0}{\sin\kappa}+z_1\cos\kappa)+2(1-\frac{v}{c}\cos\kappa)R_0\cot\kappa))} \\
&\quad\times \sum_{n=N_0-N/2}^{N_0+N/2} e^{\frac{i\omega_0\sin\kappa}{R_0c}2(z_1-y_1)(1-\frac{v}{c}\cos\kappa)x_1^n} \\
&= e^{\frac{i\omega_0\cos\kappa}{c}(2y_1-2z_1)} e^{\frac{i\omega_0\sin\kappa}{R_0c}(y_1^2-z_1^2+(z_1-y_1)(\frac{v}{c}(\frac{R_0}{\sin\kappa}+z_1\cos\kappa)+2(1-\frac{v}{c}\cos\kappa)(R_0\cot\kappa+N_0\Delta x_1)))} \\
&\quad\times \sum_{n=-N/2}^{N/2} e^{\frac{i\omega_0\sin\kappa}{R_0c}2(z_1-y_1)(1-\frac{v}{c}\cos\kappa)n\Delta x_1}.
\end{aligned} \tag{3.11}
$$

Two observations can immediately be made. First, the factor in front of the sum in formula (3.11) has magnitude one and can be left out of consideration when analyzing the SAR resolution. Second, the effect of the antenna displacement during the round-trip travel time between the orbit and the ground is accounted for by the factor $(1-\frac{v}{c}\cos\kappa)$ in the exponent under the sum in formula (3.11). To actually estimate the azimuthal resolution, one needs to compute the sum:

$$W_A(\boldsymbol{y},\boldsymbol{z}) \propto \sum_{n=-N/2}^{N/2} e^{\frac{i\omega_0 \sin\kappa}{R_0 c} 2(z_1-y_1)(1-\frac{v}{c}\cos\kappa)n\Delta x_1}. \tag{3.12}$$

This sum can be interpreted as the discrete (inverse) Fourier transform which, for example, is encountered frequently in the analysis of finite-difference approximations (see, e.g., [13]) as well as in a variety of other contexts. Sum (3.12) is a geometric sequence and can therefore be evaluated easily. Again, up to a factor of magnitude one we have

$$W_A(\boldsymbol{y},\boldsymbol{z}) \propto \frac{\sin\left[\frac{\omega_0 \sin\kappa}{R_0 c}(z_1-y_1)(1-\frac{v}{c}\cos\kappa)(N+1)\Delta x_1\right]}{\sin\left[\frac{\omega_0 \sin\kappa}{R_0 c}(z_1-y_1)(1-\frac{v}{c}\cos\kappa)\Delta x_1\right]}. \tag{3.13}$$

Let us further assume that

$$|z_1-y_1| \ll \frac{R_0 c}{\omega_0 \sin\kappa \Delta x_1} = \frac{R_0\lambda}{2\pi \sin\kappa \Delta x_1},$$

which simply means that for the purpose of conducting the analysis we would like the reference point to be sufficiently close to the target. In this case the argument of the sine function in the denominator of (3.13) is small, and we can write

$$W_A(\boldsymbol{y},\boldsymbol{z}) \propto (N+1)\,\mathrm{sinc}\left[\frac{\omega_0 \sin\kappa}{R_0 c}(z_1-y_1)\left(1-\frac{v}{c}\cos\kappa\right)(N+1)\Delta x_1\right]. \tag{3.14}$$

The sinc function (3.14) is what one typically gets instead of the ideal $\delta(z_1-y_1)$ when analyzing radar performance. The sharper the maximum of the sinc, i.e., the closer it is to the delta-function, the better the resolution of the SAR, i.e., the minimum distance between the two point targets that the radar can still tell apart. Therefore, it is natural to estimate the resolution as the width of the main lobe of the sinc,[3]

$$(z_1-y_1)\left(1-\frac{v}{c}\cos\kappa\right) = \frac{2\pi R_0 c}{\omega_0 \sin\kappa (N+1)\Delta x_1} = \frac{R_0\lambda}{\sin\kappa (N+1)\Delta x_1} \approx \frac{L\sin\kappa}{2},$$

so that we can write $(v/c \ll 1)$

$$z_1 - y_1 \approx \frac{L\sin\kappa}{2}\left(1+\frac{v}{c}\cos\kappa\right). \tag{3.15}$$

If not for the additional factor $\left(1+\frac{v}{c}\cos\kappa\right)$, formula (3.15) would yield a standard expression for the azimuthal SAR resolution in the framework of the start-stop approximation (in the

[3]Sometimes, it is taken as half this width.

squinted stripmap mode). The additional factor disappears when $\kappa = \pi/2$. In other words, in the case of broadside imaging, the start-stop approximation does not affect the azimuthal resolution of a SAR sensor at all. Otherwise, when $\cos\kappa \neq 0$, the foregoing analysis indicates that the actual resolution may be slightly worse than that obtained with the help of the start-stop approximation. The deterioration, however, is minute, on the order of v/c, which is about $2.7 \cdot 10^{-5}$ for low orbit satellites, and which can be safely disregarded for all practical purposes.

3.2. Range resolution. To analyze the range resolution, we substitute the envelope A of the chirp (see (2.1)) into formula (3.3),

$$W_R(\boldsymbol{y},\boldsymbol{z}) = \int_{-\tau/2+\tau_{\min}}^{\tau/2+\tau_{\max}} \overline{e^{i\alpha(t-|\tilde{\boldsymbol{x}}^0-\boldsymbol{y}|/c-|\boldsymbol{y}-\boldsymbol{x}^0|/c)^2}} e^{i\alpha(t-|\tilde{\boldsymbol{x}}^0-\boldsymbol{z}|/c-|\boldsymbol{z}-\boldsymbol{x}^0|/c)^2} dt, \tag{3.16}$$

where

$$\tau_{\max} = \max\{(|\tilde{\boldsymbol{x}}^0-\boldsymbol{y}|/c+|\boldsymbol{y}-\boldsymbol{x}^0|/c),(|\tilde{\boldsymbol{x}}^0-\boldsymbol{z}|/c+|\boldsymbol{z}-\boldsymbol{x}^0|/c)\} \tag{3.17a}$$

and

$$\tau_{\min} = \min\{(|\tilde{\boldsymbol{x}}^0-\boldsymbol{y}|/c+|\boldsymbol{y}-\boldsymbol{x}^0|/c),(|\tilde{\boldsymbol{x}}^0-\boldsymbol{z}|/c+|\boldsymbol{z}-\boldsymbol{x}^0|/c)\}. \tag{3.17b}$$

Formula (3.16) holds provided that $\Delta\tau \stackrel{\text{def}}{=} \tau_{\max} - \tau_{\min} < \tau$; otherwise the integral is equal to zero. If it is not zero, then from (3.16) we find

$$\begin{aligned} W_R(\boldsymbol{y},\boldsymbol{z}) &= e^{i\alpha((|\tilde{\boldsymbol{x}}^0-\boldsymbol{z}|/c+|\boldsymbol{z}-\boldsymbol{x}^0|/c)^2-(|\tilde{\boldsymbol{x}}^0-\boldsymbol{y}|/c+|\boldsymbol{y}-\boldsymbol{x}^0|/c)^2)} \\ &\times \int_{-\tau/2+\tau_{\max}}^{\tau/2+\tau_{\min}} e^{2i\alpha t((|\tilde{\boldsymbol{x}}^0-\boldsymbol{y}|/c+|\boldsymbol{y}-\boldsymbol{x}^0|/c)-(|\tilde{\boldsymbol{x}}^0-\boldsymbol{z}|/c+|\boldsymbol{z}-\boldsymbol{x}^0|/c))} dt. \end{aligned} \tag{3.18}$$

The factor in front of the integral in (3.18) can be disregarded because it has magnitude one. The integral itself needs to be evaluated for the case when the reference location $\boldsymbol{y}$ is close to the target $\boldsymbol{z}$; then, the length of the interval of integration, $\tau + \tau_{\min} - \tau_{\max} = \tau - \Delta\tau$, will also be close to τ. The integration yields

$$\begin{aligned} W_R(\boldsymbol{y},\boldsymbol{z}) &\propto \frac{c}{2i\alpha((|\tilde{\boldsymbol{x}}^0-\boldsymbol{y}|+|\boldsymbol{y}-\boldsymbol{x}^0|)-(|\tilde{\boldsymbol{x}}^0-\boldsymbol{z}|+|\boldsymbol{z}-\boldsymbol{x}^0|))} \\ &\times e^{2i\alpha t((|\tilde{\boldsymbol{x}}^0-\boldsymbol{y}|/c+|\boldsymbol{y}-\boldsymbol{x}^0|/c)-(|\tilde{\boldsymbol{x}}^0-\boldsymbol{z}|/c+|\boldsymbol{z}-\boldsymbol{x}^0|/c))}\Big|_{-\tau/2+\tau_{\max}}^{\tau/2+\tau_{\min}} \end{aligned}$$

or, equivalently (up to another factor of magnitude one),

$$\begin{aligned} W_R(\boldsymbol{y},\boldsymbol{z}) &\propto \frac{c}{2i\alpha((|\tilde{\boldsymbol{x}}^0-\boldsymbol{y}|+|\boldsymbol{y}-\boldsymbol{x}^0|)-(|\tilde{\boldsymbol{x}}^0-\boldsymbol{z}|+|\boldsymbol{z}-\boldsymbol{x}^0|))} \\ &\times e^{2i\alpha t((|\tilde{\boldsymbol{x}}^0-\boldsymbol{y}|/c+|\boldsymbol{y}-\boldsymbol{x}^0|/c)-(|\tilde{\boldsymbol{x}}^0-\boldsymbol{z}|/c+|\boldsymbol{z}-\boldsymbol{x}^0|/c))}\Big|_{-\tau/2+\Delta\tau/2}^{\tau/2-\Delta\tau/2} \\ &= \frac{2c\tau}{B((|\tilde{\boldsymbol{x}}^0-\boldsymbol{y}|+|\boldsymbol{y}-\boldsymbol{x}^0|)-(|\tilde{\boldsymbol{x}}^0-\boldsymbol{z}|+|\boldsymbol{z}-\boldsymbol{x}^0|))} \\ &\times \sin\left(\frac{B((|\tilde{\boldsymbol{x}}^0-\boldsymbol{y}|+|\boldsymbol{y}-\boldsymbol{x}^0|)-(|\tilde{\boldsymbol{x}}^0-\boldsymbol{z}|+|\boldsymbol{z}-\boldsymbol{x}^0|))}{2c} \pm \frac{B\Delta\tau^2}{2\tau}\right), \end{aligned} \tag{3.19}$$

where B is the bandwidth of the chirp (see (2.2)) and the sign plus or minus under the sine function in (3.19) depends on what actual value delivers the maximum and minimum in formulae (3.17a) and (3.17b). In any event, as we are primarily interested in the case $\Delta\tau/\tau \ll 1$, we can disregard the second term under the sine and obtain

$$W_R(\boldsymbol{y},\boldsymbol{z}) \propto \tau \cdot \operatorname{sinc}\left(\frac{B((|\tilde{\boldsymbol{x}}^0-\boldsymbol{y}|+|\boldsymbol{y}-\boldsymbol{x}^0|)-(|\tilde{\boldsymbol{x}}^0-\boldsymbol{z}|+|\boldsymbol{z}-\boldsymbol{x}^0|))}{2c}\right). \tag{3.20}$$

If the receiving location $\tilde{\boldsymbol{x}}^0$ coincides with the emitting location $\boldsymbol{x}^0$, which corresponds to the start-stop approximation, then formula (3.20) yields a standard expression for the range resolution, i.e., for the resolution of the distance between the antenna and the target. It is given by the full width of the main lobe of the sinc, which is twice its half-width, and the latter is obtained by setting the argument of the sinc equal to π:

$$|\boldsymbol{x}^0-\boldsymbol{y}|-|\boldsymbol{x}^0-\boldsymbol{z}| = \frac{2\pi c}{B}. \tag{3.21}$$

If the emitting and receiving locations are different, then instead of (3.21) we have

$$(|\tilde{\boldsymbol{x}}^0-\boldsymbol{y}|+|\boldsymbol{y}-\boldsymbol{x}^0|)-(|\tilde{\boldsymbol{x}}^0-\boldsymbol{z}|+|\boldsymbol{z}-\boldsymbol{x}^0|) = \frac{4\pi c}{B}. \tag{3.22}$$

Formula (3.21) can be interpreted as if the target $\boldsymbol{z}$ and the reference location $\boldsymbol{y}$ lie on two concentric spheres centered at $\boldsymbol{x}^0$, and these two spheres can be told apart if their radii differ by more than $2\pi c/B$. Likewise, formula (3.22) shall be interpreted as if the target $\boldsymbol{z}$ and the reference location $\boldsymbol{y}$ lie on two ellipsoids of revolution with common foci $\boldsymbol{x}^0$ and $\tilde{\boldsymbol{x}}^0$, and these two ellipsoids can be told apart if the corresponding sums of distances to the foci (each sum is equal to twice the major semiaxis) differ by more than $4\pi c/B$.

Hence, the eccentricity of the ellipsoids in (3.22) will provide a measure of the difference between the resolution obtained using the start-stop approximation and the resolution obtained with no use of this approximation. It turns out that this eccentricity is extremely close to one, i.e., that the ellipsoids are almost indistinguishable from spheres. Indeed, if the major semiaxis is estimated as $a = R_0 \approx 1000km$, then the minor semiaxis is $b = \sqrt{R_0^2-(vT/2)^2} \approx R_0(1-(vT)^2/8R_0^2) \approx R_0(1-2\cdot 10^{-10})$, because $vT \approx 40m$. With the chirp bandwidth $B \gtrsim 10^7 Hz$, the resolution given by either (3.21) or (3.22) appears to be on the order of meters, whereas the correction due to the eccentricity will be fractions of a millimeter. Clearly, this correction can be disregarded, which altogether means that in practice the displacement of the antenna during the round-trip travel time between the orbit and the Earth does not affect the resolution of a spaceborne SAR sensor.

4. The Doppler effect. In section 3, we do take into account that the antenna changes its position as the signal it emits travels to the target and back. We still assume, though, that the antenna is motionless during the time the signal is emitted and the scattered response is received. In reality, however, the antenna is moving continuously. Therefore, the expressions for the emitted and scattered field that we employed for constructing the generalized ambiguity function in section 2 may themselves need to be corrected. In particular, expression (2.3) yields the field emitted by a motionless antenna; it will need to be modified to account for the

actual motion. Likewise, expression (2.7) yields the scattered field in the original motionless coordinate system; it will need to be modified because the field is received by a moving antenna.

In this section, we will use the Lorentz transform to address the fact that the antenna is moving. We will see, in particular, that once the motion of the wave's emitter and/or receiver is properly accounted for, the observable frequency of the signal changes. This phenomenon is known as the Doppler frequency shift; see, e.g., [10] for electromagnetic waves and [11] for acoustics. In the literature on SAR, this frequency shift is sometimes used to explain the mechanism of azimuthal resolution, because the sequence of signals that illuminate the target from different emitting positions along the orbit can be interpreted as a linear chirp; see, e.g., [8]. A relation between the Doppler approach and that often used in tomography has also been established [1, 12]. However, in the rigorous analysis based on the generalized ambiguity function, the Doppler effect is often disregarded. We, on the other hand, will show that the Doppler frequency shift should be included into the definition of a matched filter so as to minimize the distortions of the image.

Let us assume that the antenna is engaged in a straightforward uniform motion along the coordinate "1" of a Cartesian coordinate system and that the speed of motion is v; see Figure 1. Of course, strictly speaking, this is not true for a satellite orbiting the Earth, but it is a sufficiently good approximation for short stretches of the orbit. We will denote the position of the antenna by $\boldsymbol{x} = \boldsymbol{x}(t) = (vt, H, 0)$, where H is the orbit altitude (see Figure 1), and we will also assume that the pointwise antenna emits a signal $P(t)$. To find the corresponding field $\varphi(t, \boldsymbol{z})$ as a function of the time t and the observer's (target) location $\boldsymbol{z}$, we first change the coordinates so that in the new frame the antenna becomes motionless. Using the standard notation for the relativistic square root, $\beta = \sqrt{1 - v^2/c^2}$, where c is the propagation speed, we write

$$\theta = \frac{t}{\beta} - \frac{v/c}{\beta}\frac{z_1}{c}, \tag{4.1a}$$

$$\zeta_1 = -\frac{v/c}{\beta}ct + \frac{z_1}{\beta}. \tag{4.1b}$$

The remaining two spatial coordinates, z_2 and z_3, do not change, so that the overall transformation is $(t, z_1, z_2, z_3) \mapsto (\theta, \zeta_1, z_2, z_3)$. It is known as the Lorentz transform, and its distinctive feature is that it preserves the form of the d'Alembert operator [9, Chapter 3, section 3]. In particular, the equation

$$\begin{aligned} &\frac{1}{c^2}\frac{\partial^2\varphi}{\partial t^2} - \frac{\partial^2\varphi}{\partial z_1^2} - \frac{\partial^2\varphi}{\partial z_2^2} - \frac{\partial^2\varphi}{\partial z_3^2} \\ &\qquad = P(t)\delta(\boldsymbol{z} - \boldsymbol{x}(t)) \equiv P(t)\delta(z_1 - vt)\delta(z_2 - H)\delta(z_3) \end{aligned} \tag{4.2a}$$

becomes

$$\begin{aligned} &\frac{1}{c^2}\frac{\partial^2\varphi}{\partial\theta^2} - \frac{\partial^2\varphi}{\partial\zeta_1^2} - \frac{\partial^2\varphi}{\partial z_2^2} - \frac{\partial^2\varphi}{\partial z_3^2} \\ &\qquad = P\left(\frac{\theta}{\beta} + \frac{v/c}{\beta}\frac{\zeta_1}{c}\right)\delta(\beta\zeta_1)\delta(z_2 - H)\delta(z_3) \stackrel{\text{def}}{=} f(\theta, \zeta_1, z_2, z_3). \end{aligned} \tag{4.2b}$$

Note that if the standard Galileo transform were used instead of (4.1), then the differential operator in (4.2b) would not have been the same as in (4.2a), even though the antenna would still have been motionless in the new frame. The solution of (4.2b) subject to zero initial conditions can be easily found with the help of the Kirchhoff integral in the new coordinates:

$$\varphi(\theta,\zeta_1,z_2,z_3)=\frac{1}{4\pi}\iiint_{\rho'\le c\theta}\frac{f(\theta-\rho'/c,\zeta_1',z_2',z_3')}{\rho'}d\zeta_1'dz_2'dz_3'=\frac{1}{4\pi\beta}\frac{P((\theta-\rho/c)/\beta)}{\rho}, \tag{4.3}$$

where $\rho'=\sqrt{(\zeta_1-\zeta_1')^2+(z_2-z_2')^2+(z_3-z_3')^2}$ and $\rho=\sqrt{\zeta_1^2+(z_2-H)^2+z_3^2}$. Note that up to the relativistic factors β, solution (4.3) is a standard retarded potential (compare with formula (2.3)) from the point source located at $(0,H,0)$ in the new coordinates, which is expected. Note also that as an alternative, solution (4.3) could have been obtained in a "brute force" way, by computing the convolution with the fundamental solution of (4.2a) in the original coordinates; see Appendix A.

To understand the Doppler effect, solution (4.3) needs to be cast back to the original coordinates. Let us denote $r=\sqrt{z_1^2+(z_2-H)^2+z_3^2}$. Then, according to (4.1b), we can write

$$\begin{aligned}\zeta_1^2&=\frac{1}{\beta^2}(z_1-vt)^2=\frac{1}{\beta^2}(z_1^2-2z_1vt+(vt)^2)=z_1^2+\frac{1-\beta^2}{\beta^2}z_1^2+\frac{1}{\beta^2}(-2z_1vt+(vt)^2)\\&=z_1^2-2z_1vt+\frac{1-\beta^2}{\beta^2}(z_1-vt)^2+(vt)^2=z_1^2-2rvt\cos\gamma+\frac{1-\beta^2}{\beta^2}(z_1-vt)^2+(vt)^2,\end{aligned}$$

where, as before (in section 3), γ denotes the angle between the velocity $\boldsymbol{v}$ (positive first coordinate) and the direction from the antenna to the target; see Figure 1. Consequently,

$$\rho^2=r^2-2rvt\cos\gamma+(vt)^2+\frac{1-\beta^2}{\beta^2}(z_1-vt)^2. \tag{4.4}$$

The last term in equality (4.4) is $\sim v^2/c^2$, where v/c itself is small, $v/c\ll 1$. The second to last term is also quadratic with respect to v/c for the times of interest $t\sim r/c$. Hence, for the values of γ away from $\pi/2$ (so that $\cos\gamma\neq 0$), these two terms can be dropped, which yields the following approximate expression:

$$\rho\approx\sqrt{r^2-2rvt\cos\gamma}=r\sqrt{1-\frac{2vt}{r}\cos\gamma}\approx r-vt\cos\gamma. \tag{4.5}$$

Then, substituting the value of ρ given by (4.5) into the solution (4.3), using the definition of the Lorentz transform (4.1), and approximating $1/\beta=(1-v^2/c^2)^{-1/2}\approx 1+v^2/2c^2\approx 1$, we arrive at

$$\varphi(t,\boldsymbol{z})\approx\frac{1}{4\pi\beta}\frac{P\left(\frac{1}{\beta}\left(t-\frac{vz_1}{c^2}\right)-\frac{r}{c}+\frac{v}{c}t\cos\gamma\right)}{\rho}\approx\frac{1}{4\pi}\frac{P\left(\left(t-\frac{r}{c}\right)\left(1+\frac{v}{c}\cos\gamma\right)\right)}{\rho}. \tag{4.6}$$

If the function $P(t)$ is a fast oscillation with the frequency ω_0, then it is also possible to replace ρ by r in the denominator of (4.6) because it amounts to only a slow and small ($\sim v/c$) variation of the amplitude:

$$\varphi(t,\boldsymbol{z})\approx\frac{1}{4\pi}\frac{P\left(\left(t-\frac{r}{c}\right)\left(1+\frac{v}{c}\cos\gamma\right)\right)}{r}. \tag{4.7}$$

Formula (4.7) is almost the standard retarded potential, except for the correction factor $1+\frac{v}{c}\cos\gamma$ inside $P(\,\cdot\,)$. The presence of this factor means that if the field emitted by a moving antenna is received at a motionless target, then the frequency measured at the target changes; instead of the original ω_0, it becomes $\omega_0\left(1+\frac{v}{c}\cos\gamma\right)$. This implies the increase of the frequency if the antenna is moving toward the target, $0\le\gamma<\pi/2$, and the decrease of the frequency if the antenna is moving away from the target, $\pi/2<\gamma\le\pi$. The correction to the frequency is linear with respect to v/c (since we have dropped the quadratic terms $\sim v^2/c^2$ in our analysis), and, accordingly, the foregoing phenomenon is called the linear Doppler effect or linear Doppler frequency shift. Note also that in the same linear framework we can recast formula (4.7) as

$$\varphi(t,\boldsymbol{z})\approx\frac{1}{4\pi r}P\left(\frac{t-\frac{r}{c}}{1-\frac{v}{c}\cos\gamma}\right). \tag{4.8}$$

Expression (4.8) can be obtained independently after (4.2a) has been solved directly by computing the convolution with the fundamental solution; see Appendix A.

For the sake of completeness, let us also comment briefly on the quadratic Doppler effect. The last two terms that we have disregarded on the right-hand side of (4.4) become important, i.e., comparable to the second term, if $\cos\gamma\sim v/c$ or, equivalently, $\pi/2-v/c\lesssim\gamma\lesssim\pi/2+v/c$, where $v/c\ll1$. This means that the quadratic effect can manifest itself only for the broadside imaging, when the direction of the beam is normal to the orbit. On top of that, it may be noticeable only in a very narrow central part of the beam, because in practice $v/c\sim10^{-5}$, whereas the angular semiwidth of the beam λ/L could be about $1/30$ for the wavelength $\lambda=30cm$ (corresponding to the carrier frequency $\omega_0=1GHz$) and the antenna size $L=10m$. Hereafter, the quadratic Doppler effect $\sim v^2/c^2\sim10^{-10}$ will be neglected.

To account for the linear Doppler effect when building the generalized ambiguity function, we replace formula (2.3) with formula (4.7). Then, we differentiate $\varphi(t,\boldsymbol{z})$ and thus derive the sources of the scattered field in the framework of the first Born approximation (cf. formula (2.5)):

$$\frac{\partial^2\varphi}{\partial t^2}(t,\boldsymbol{z})\approx-\frac{\omega_0^2\left(1+\frac{v}{c}\cos\gamma\right)^2}{4\pi}\frac{P\left(\left(t-\frac{r}{c}\right)\left(1+\frac{v}{c}\cos\gamma\right)\right)}{r}. \tag{4.9}$$

For the point target located at $\boldsymbol{z}$, the scattered wave at $(t,\boldsymbol{x})$ is a retarded potential centered at $\boldsymbol{z}$ and modulated by the function (4.9) as a function of time (cf. formula (2.7)):

$$\psi(t,\boldsymbol{x})=-\frac{\omega_0^2\left(1+\frac{v}{c}\cos\gamma\right)^2}{16\pi^2}\frac{P\left(\left(t-\frac{|\boldsymbol{x}-\boldsymbol{z}|}{c}-\frac{r}{c}\right)\left(1+\frac{v}{c}\cos\gamma\right)\right)}{r\cdot|\boldsymbol{x}-\boldsymbol{z}|}. \tag{4.10}$$

When the scattered pulse (4.10) travels back from the target to the antenna, it generates another contribution to the Doppler frequency shift. The corresponding analysis can be conducted as before, by going to the frame of reference in which the receiver (antenna) is motionless. To do so, we employ essentially the same Lorentz transform except that as we want the solution in the form of a retarded potential centered around the origin, we need to have the origin of the new system initially located at the target $\boldsymbol{z}$, rather than at $\boldsymbol{x}(0)=(0,H,0)$.

As the scattered field is received at the antenna $\boldsymbol{x}$, we will use the variables $\boldsymbol{x} = (x_1, x_2, x_3)$ to write the transform, whereas the location of the target $\boldsymbol{z} = (z_1, z_2, z_3)$ will be considered fixed (cf. formulae (4.1)):

$$\hat{\theta} = \frac{t}{\beta} - \frac{v/c}{\beta}\frac{x_1 - z_1}{c}, \tag{4.11a}$$

$$\xi_1 = -\frac{v/c}{\beta}ct + \frac{x_1 - z_1}{\beta}. \tag{4.11b}$$

Similarly to (4.1), the remaining two spatial coordinates do not get changed so that altogether we have the transformation $(t, x_1, x_2, x_3) \mapsto (\hat{\theta}, \xi_1, x_2, x_3)$. Relation (4.11b) implies, in particular, that in the new coordinates the antenna is not moving, because $x_1 = vt$ corresponds to $\xi_1 = -z_1/\beta = \text{const}$.

We introduce

$$\hat{\rho} = \sqrt{\xi_1^2 + (x_2 - z_2)^2 + (x_3 - z_3)^2}$$

and

$$\hat{r} = \sqrt{(x_1 - z_1)^2 + (x_2 - z_2)^2 + (x_3 - z_3)^2} = |\boldsymbol{x} - \boldsymbol{z}|.$$

Then, $x_1 - z_1 = -\hat{r}\cos\gamma$ (see Figure 1), and repeating the same derivation that led us to formula (4.5), we arrive at the following linearized relation between the distances:

$$\hat{\rho} \approx \hat{r} + vt\cos\gamma. \tag{4.12}$$

Consequently, letting $\beta \approx 1$ and using (4.11b), we can write

$$\begin{aligned}\hat{\rho}\cos\gamma &\approx \hat{r}\cos\gamma + vt\cos^2\gamma = -(x_1 - z_1) + vt\cos^2\gamma \\ &\approx -\xi_1 - vt + vt\cos^2\gamma = -\xi - vt\sin^2\gamma\end{aligned}$$

so that

$$\xi_1 = -\hat{\rho}\cos\gamma - vt\sin^2\gamma. \tag{4.13}$$

Next, using formula (4.11a) and again neglecting quadratic terms with respect to v/c, we obtain from (4.12)

$$\hat{r} \approx \hat{\rho} - vt\cos\gamma = \hat{\rho} - v\beta\hat{\theta}\cos\gamma - \frac{v^2}{c^2}(x_1 - z_1) \approx \hat{\rho} - v\hat{\theta}\cos\gamma. \tag{4.14}$$

Finally, to implement the transformation in formula (4.10), we have to transform all times and distances on its right-hand side to new coordinates. We note that formula (4.10) is written so that $\boldsymbol{x}$ can be any location in space. We, however, are interested only in the case when $\boldsymbol{x}$ is the location of the antenna. Since the displacement of the antenna during the round-trip travel time of the signal does not affect the performance of the radar (section 3), we take $\boldsymbol{x} = \boldsymbol{x}(0) = (0, H, 0)$. In this case, $\hat{r} = |\boldsymbol{x} - \boldsymbol{z}| = r$, and instead of (4.10) we can write

$$\psi(t, \boldsymbol{x}) = -\frac{\omega_0^2\left(1 + \frac{v}{c}\cos\gamma\right)^2}{16\pi^2}\frac{P\left(\left(t - \frac{2\hat{r}}{c}\right)\left(1 + \frac{v}{c}\cos\gamma\right)\right)}{\hat{r}^2}. \tag{4.15}$$

Substituting $\hat{r}$ given by (4.14) into formula (4.15), and also substituting the following expression for t, which is derived by inverting (4.11) and then using (4.13),

$$t = \frac{\hat{\theta}}{\beta} + \frac{v/c}{\beta}\frac{\xi_1}{c} \approx \hat{\theta} - \frac{v}{c}\frac{\hat{\rho}}{c}\cos\gamma,$$

we have

$$\begin{aligned}\psi(\hat{\theta},\xi_1,x_2,x_3) &= -\frac{\omega_0^2\left(1+\frac{v}{c}\cos\gamma\right)^2}{16\pi^2}\frac{P\left(\left(\hat{\theta}-\frac{2\hat{\rho}}{c}\right)\left(1+\frac{v}{c}\cos\gamma\right)^2\right)}{\hat{r}^2}\\ &\approx -\frac{\omega_0^2\left(1+2\frac{v}{c}\cos\gamma\right)}{16\pi^2}\frac{P\left(\left(\hat{\theta}-\frac{2\hat{\rho}}{c}\right)\left(1+2\frac{v}{c}\cos\gamma\right)\right)}{\hat{r}^2}\\ &\approx -\frac{\omega_0^2}{16\pi^2}\frac{P\left(\left(\hat{\theta}-\frac{2\hat{\rho}}{c}\right)\left(1+2\frac{v}{c}\cos\gamma\right)\right)}{\hat{\rho}^2},\end{aligned} \tag{4.16}$$

where the last equality in (4.16) was obtained as before, by disregarding a slow and small ($\sim v/c$) variation in the amplitude. Formula (4.16) indicates, in particular, that in the frame of reference in which the satellite is motionless, the observed frequency of the signal emitted by the antenna, scattered off the target, and then again received by the antenna is $\omega_0\left(1+2\frac{v}{c}\cos\gamma\right)$, compared to the original frequency ω_0. Otherwise, if not for the coordinate change and the additional amplitude factor, the solution (4.16) looks exactly the same as it would have looked if both the antenna and the target were motionless (cf. formula (2.7)), with $\frac{2\hat{\rho}}{c}$ being the round-trip travel time between the antenna and the target. Hence, this scattered solution can be used for building the generalized ambiguity function in the new coordinates.

4.1. Azimuthal resolution. Hereafter, we will follow the path of section 2 for constructing the generalized ambiguity function. In doing so, we will use solution (4.16) instead of (2.7) as the central "building block." Following the analysis of section 3, we will also disregard the displacement of the antenna from the very beginning. For the azimuthal factor we can then write (cf. formula (3.2))

$$W_A(\boldsymbol{y},\boldsymbol{z}) = \sum_n \vartheta(\boldsymbol{z},\boldsymbol{x}^n)e^{2i\omega_0\left(|\boldsymbol{x}^n-\boldsymbol{y}|\left(1+\frac{2v}{c}\cos\gamma_{\boldsymbol{y}}^n\right)-|\boldsymbol{x}^n-\boldsymbol{z}|\left(1+\frac{2v}{c}\cos\gamma_{\boldsymbol{z}}^n\right)\right)/c}, \tag{4.17}$$

where the distances $|\boldsymbol{x}^n-\boldsymbol{y}|$ and $|\boldsymbol{x}^n-\boldsymbol{z}|$, even though denoted the same way as before, shall be measured in the Lorentz transformed coordinates, in which the antenna is not moving,[4] and the notation for the angles, $\gamma_{\boldsymbol{y}}^n$ and $\gamma_{\boldsymbol{z}}^n$, indicates that they depend on the position of the antenna.

We are particularly interested in analyzing that part of the exponent in formula (4.17)

[4]This applies to all other distances that appear in subsequent derivations in this section.

which has the factor v/c in front of it:

$$\begin{aligned}&\frac{2i\omega_0}{c}\frac{2v}{c}\left(|\boldsymbol{x}^n-\boldsymbol{y}|\cos\gamma_{\boldsymbol{y}}^n-|\boldsymbol{x}^n-\boldsymbol{z}|\cos\gamma_{\boldsymbol{z}}^n\right)\\ =\frac{2i\omega_0}{c}\frac{2v}{c}&\left(\frac{R_0}{\sin\kappa}(\cos\gamma_{\boldsymbol{y}}^n-\cos\gamma_{\boldsymbol{z}}^n)+\frac{(y_1-q_1^n)^2\sin\kappa}{2R_0}\cos\gamma_{\boldsymbol{y}}^n-\frac{(z_1-q_1^n)^2\sin\kappa}{2R_0}\cos\gamma_{\boldsymbol{z}}^n\right.\\ &\left.+(y_1-q_1^n)\cos\kappa\cos\gamma_{\boldsymbol{y}}^n-(z_1-q_1^n)\cos\kappa\cos\gamma_{\boldsymbol{z}}^n\right).\end{aligned}$$

Note that the previous formula was derived with the help of (3.4). To simplify subsequent analysis, we will assume that the imaging is broadside, i.e., $\kappa=\pi/2$; see Figure 1. Then,

$$\begin{aligned}&\frac{2i\omega_0}{c}\frac{2v}{c}\left(|\boldsymbol{x}^n-\boldsymbol{y}|\cos\gamma_{\boldsymbol{y}}^n-|\boldsymbol{x}^n-\boldsymbol{z}|\cos\gamma_{\boldsymbol{z}}^n\right)\\ =\frac{2i\omega_0}{c}\frac{2v}{c}&\left(R_0(\cos\gamma_{\boldsymbol{y}}^n-\cos\gamma_{\boldsymbol{z}}^n)+\frac{(y_1-q_1^n)^2}{2R_0}\cos\gamma_{\boldsymbol{y}}^n-\frac{(z_1-q_1^n)^2}{2R_0}\cos\gamma_{\boldsymbol{z}}^n\right).\end{aligned}$$

Besides, as the antenna beam is narrow, we can also say that both $\gamma_{\boldsymbol{y}}^n$ and $\gamma_{\boldsymbol{z}}^n$ are close to $\pi/2$ so that

$$\cos\gamma_{\boldsymbol{y}}^n\approx\cot\gamma_{\boldsymbol{y}}^n=\frac{y_1-q_1^n}{R_0}\quad\text{and}\quad\cos\gamma_{\boldsymbol{z}}^n\approx\cot\gamma_{\boldsymbol{z}}^n=\frac{z_1-q_1^n}{R_0}.$$

Hence, we have

$$\begin{aligned}&\frac{2i\omega_0}{c}\frac{2v}{c}\left(|\boldsymbol{x}^n-\boldsymbol{y}|\cos\gamma_{\boldsymbol{y}}^n-|\boldsymbol{x}^n-\boldsymbol{z}|\cos\gamma_{\boldsymbol{z}}^n\right)\\ \approx\frac{2i\omega_0}{R_0c}\frac{2v}{c}&\left(R_0(y_1-z_1)+\frac{(y_1-q_1^n)^3}{2R_0}-\frac{(z_1-q_1^n)^3}{2R_0}\right).\end{aligned}\tag{4.18}$$

The key consideration regarding the previous formula is that the first term in the brackets on its right-hand side does not depend on n. Consequently, when expression (4.18) is substituted back into the exponent in formula (4.17), the corresponding factor can be taken outside the sum and disregarded because its magnitude will be equal to one. Therefore, formula (4.17) will eventually simplify to (cf. formula (3.7))

$$W_A(\boldsymbol{y},\boldsymbol{z})\propto\sum_{n=N_0-N/2}^{N_0+N/2}e^{\frac{2i\omega_0}{R_0c}\left((z_1-y_1)q_1^n+\frac{v}{c}\frac{(y_1-q_1^n)^3}{R_0}-\frac{v}{c}\frac{(z_1-q_1^n)^3}{R_0}\right)}.\tag{4.19}$$

It is clear that the second and third terms in the exponent on the right-hand side of formula (4.19) are much smaller than the first term, because in addition to the small factor v/c they contain another small factor $(y_1-q_1^n)/R_0\sim(z_1-q_1^n)/R_0\sim\lambda/L$. Dropping these two terms, we obtain (cf. formula (3.12))

$$W_A(\boldsymbol{y},\boldsymbol{z})\propto\sum_{n=-N/2}^{N/2}e^{\frac{2i\omega_0}{R_0c}(z_1-y_1)n\Delta x_1}.\tag{4.20}$$

Formula (4.20) provides a conventional expression for the azimuthal component of the generalized ambiguity function[5]; see, e.g., [4]. Once the sum on the right-hand side is evaluated, it yields the azimuthal resolution

$$z_1 - y_1 \approx \frac{L}{2}, \tag{4.21}$$

which is standard in the analysis of SAR performance (note that formula (3.15) reduces to (4.21) for $\kappa = \pi/2$). Formula (4.21) shows that if the reference distance $|\boldsymbol{x}^n - \boldsymbol{y}|$ in the exponent in formula (4.17) is taken with the Doppler correction, i.e., if the frequency shift is included in the definition of a matched filter, then the azimuthal resolution of the radar stays basically unaffected.

Let us now see what will change if the matched filter is taken with no Doppler correction. In this case, instead of formula (4.17) we have

$$W_A(\boldsymbol{y},\boldsymbol{z}) = \sum_n \vartheta(\boldsymbol{z},\boldsymbol{x}^n) e^{2i\omega_0\left(|\boldsymbol{x}^n-\boldsymbol{y}|-|\boldsymbol{x}^n-\boldsymbol{z}|\left(1+\frac{2v}{c}\cos\gamma_{\boldsymbol{z}}^n\right)\right)/c}, \tag{4.22}$$

and, consequently, the additional terms in the exponent of (4.22) are (cf. formula (4.18))

$$-\frac{2i\omega_0}{c}\frac{2v}{c}|\boldsymbol{x}^n-\boldsymbol{z}|\cos\gamma_{\boldsymbol{z}}^n \approx -\frac{2i\omega_0}{R_0 c}\frac{2v}{c}\left(R_0(z_1-q_1^n)+\frac{(z_1-q_1^n)^3}{2R_0}\right). \tag{4.23}$$

The first obvious difference that we observe between formulae (4.18) and (4.23) is that the leading term in the brackets on the right-hand side of (4.23) depends on n. Hence, if we employ the same argument as before and disregard the second term on the right-hand side of (4.23), then, instead of (4.20), we will arrive at

$$\begin{aligned} W_A(\boldsymbol{y},\boldsymbol{z}) &\propto \sum_{n=-N/2}^{N/2} e^{\frac{2i\omega_0}{R_0 c}\left((z_1-y_1)+\frac{2v}{c}R_0\right)n\Delta x_1} \\ &\sim (N+1)\,\mathrm{sinc}\left[\frac{\omega_0}{R_0 c}\left((z_1-y_1)+\frac{2v}{c}R_0\right)(N+1)\Delta x_1\right]. \end{aligned} \tag{4.24}$$

Formula (4.24) implies that the azimuthal resolution of the radar, per se, remains unchanged. However, the entire imaged scene gets shifted along the track (orbit) by $-\frac{2v}{c}R_0$. For the typical parameters involved, the magnitude of this spatial shift could be about 50m.

4.2. Range resolution. For the range part of the generalized ambiguity function we can write, instead of (3.16),

$$\begin{aligned} W_R(\boldsymbol{y},\boldsymbol{z}) = \int_{-\tau/2+\tau_{\max}}^{\tau/2+\tau_{\min}} & e^{-i\alpha\left(\left(t-\frac{2|\boldsymbol{x}^0-\boldsymbol{y}|}{c}\right)\left(1+\frac{2v}{c}\cos\gamma_{\boldsymbol{y}}\right)\right)^2} e^{i\alpha\left(\left(t-\frac{2|\boldsymbol{x}^0-\boldsymbol{z}|}{c}\right)\left(1+\frac{2v}{c}\cos\gamma_{\boldsymbol{z}}\right)\right)^2} \\ & \times e^{i\omega_0 t\left(\frac{2v}{c}\cos\gamma_{\boldsymbol{z}}-\frac{2v}{c}\cos\gamma_{\boldsymbol{y}}\right)}dt, \end{aligned} \tag{4.25}$$

[5]Formula (3.12) yields a somewhat more complicated expression that accounts for the displacement of the antenna.

where the last factor under the integral on the right-hand side of (4.25) appears because the Doppler correction shall be substituted not only into the slowly varying envelope $A(t)$ but also into the fast carrier oscillation $e^{i\omega_0 t}$ in the definition of the chirp (2.1). Next, we assume with no loss of generality that $\gamma_{\boldsymbol{z}} = \gamma_{\boldsymbol{y}} = \gamma$, which merely implies that the reference location $\boldsymbol{y}$ and the target $\boldsymbol{z}$ are on the same line of sight from the antenna. Then, formula (4.25) transforms into

$$W_R(\boldsymbol{y},\boldsymbol{z}) = \int_{-\tau/2+\tau_{\min}}^{\tau/2+\tau_{\max}} e^{-i\alpha\left(\left(t-\frac{2|\boldsymbol{x}^0-\boldsymbol{y}|}{c}\right)\left(1+\frac{2v}{c}\cos\gamma\right)\right)^2} e^{i\alpha\left(\left(t-\frac{2|\boldsymbol{x}^0-\boldsymbol{z}|}{c}\right)\left(1+\frac{2v}{c}\cos\gamma\right)\right)^2} dt, \tag{4.26}$$

where for the limits of integration we have (cf. formulae (3.17a), (3.17b))

$$\tau_{\max} = 2\left(1+\frac{2v}{c}\cos\gamma\right)\max\{|\boldsymbol{x}^0-\boldsymbol{y}|/c, |\boldsymbol{x}^0-\boldsymbol{z}|/c\}$$

and

$$\tau_{\min} = 2\left(1+\frac{2v}{c}\cos\gamma\right)\min\{|\boldsymbol{x}^0-\boldsymbol{y}|/c, |\boldsymbol{x}^0-\boldsymbol{z}|/c\}.$$

In the exponent in formula (4.26), we drop the terms proportional to v^2/c^2 and also disregard the terms that do not depend on t, as the latter yield only an inessential factor of magnitude one in front of the integral:

$$W_R(\boldsymbol{y},\boldsymbol{z}) \propto \int_{-\tau/2+\tau_{\min}}^{\tau/2+\tau_{\max}} e^{i\alpha t\frac{4(|\boldsymbol{x}^0-\boldsymbol{y}|-|\boldsymbol{x}^0-\boldsymbol{z}|)}{c}\left(1+\frac{4v}{c}\cos\gamma\right)} dt. \tag{4.27}$$

Then, following the same argument as in the end of section 3, we obtain (cf. formula (3.20))

$$W_R(\boldsymbol{y},\boldsymbol{z}) \propto \tau\,\mathrm{sinc}\left(\frac{B(|\boldsymbol{x}^0-\boldsymbol{y}|-|\boldsymbol{x}^0-\boldsymbol{z}|)}{c}\left(1+\frac{4v}{c}\cos\gamma\right)\right). \tag{4.28}$$

Formula (4.28) yields the range resolution

$$|\boldsymbol{x}^0-\boldsymbol{y}|-|\boldsymbol{x}^0-\boldsymbol{z}| = \frac{2\pi c}{B}\left(1-\frac{4v}{c}\cos\gamma\right), \tag{4.29}$$

which differs from the standard expression (3.21) only by the factor $\left(1-\frac{4v}{c}\cos\gamma\right)$, which is very close to one (recall that $v/c \sim 10^{-5}$). Moreover, in the case of broadside imaging we can take $\gamma = \pi/2$ so that (4.29) reduces to (3.21) and the range resolution stays completely unaffected by the Doppler frequency shift.

Next, we need to analyze the case when the matched filter is taken with no Doppler correction. Then, instead of (4.27) we obtain

$$W_R(\boldsymbol{y},\boldsymbol{z}) \propto \int_{-\tau/2+\tau_{\min}}^{\tau/2+\tau_{\max}} e^{i\alpha t\left(\frac{4(|\boldsymbol{x}^0-\boldsymbol{y}|-|\boldsymbol{x}^0-\boldsymbol{z}|)}{c}-\frac{4|\boldsymbol{x}^0-\boldsymbol{z}|}{c}\frac{4v}{c}\cos\gamma\right)+i\alpha t^2\frac{4v}{c}\cos\gamma} dt. \tag{4.30}$$

First, we notice that if $\gamma = \pi/2$ (broadside imaging), then integral (4.30) reduces to standard and yields a conventional expression for the range resolution, $|\boldsymbol{x}^0-\boldsymbol{y}|-|\boldsymbol{x}^0-\boldsymbol{z}| = \frac{2\pi c}{B}$; see

formula (3.21). Otherwise, there is an additional term in the part of the exponent in formula (4.30) that is linear with respect to t. It will cause an overall shift of the entire imaged scene by $|\boldsymbol{x}^0 - \boldsymbol{z}|\frac{4v}{c}\cos\gamma$. Generally speaking, this value may be of the same order of magnitude as that obtained for an along-the-track shift (see formula (4.24)); however, for γ close to $\pi/2$ (near broadside imaging) it becomes small.

Moreover, for $\gamma \neq \pi/2$ there remains a small quadratic term with respect to t in the exponent under the integral on the right-hand side of formula (4.30). Integrals of this type were studied in [15] in the context of SAR imaging through the Earth's ionosphere. It was shown that this quadratic term does not affect the resolution per se in the sense that the distance between the central maximum and the first minimum of the resulting ambiguity function appears exactly the same as the half-width of the corresponding sinc. However, the sharpness (contrast) of the image may be affected, because the value of the first minimum is not zero. Based on the analysis presented in [15], it is possible to show that for the range factor given by (4.30) we have

$$\frac{\min|W_R(\boldsymbol{y},\boldsymbol{z})|}{\max|W_R(\boldsymbol{y},\boldsymbol{z})|} \sim \frac{\alpha\tau^2}{2\pi^2}\frac{4v}{c}\cos\gamma = \frac{B\tau}{\pi^2}\frac{4v}{c}\cos\gamma. \tag{4.31}$$

Formula (4.31) indicates that, generally speaking, the degree to which disregarding the Doppler frequency shift may adversely affect the image depends on the waveform used for imaging. More precisely, to reduce the deterioration of the image sharpness, one has to minimize the product of the pulse bandwidth B times its length τ. Most modern SAR systems use high range-resolution pulses that have sufficiently large B (i.e., large chirp rate α; see formulae (2.1) and (2.2)); in this case, the chirp duration must be very short. It turns out that for the typical values of the parameters, $B = 10MHz$ and $\tau = 5\cdot 10^{-5}$sec, the degradation of the image is indeed negligible because the right-hand side of (4.31) is $\sim 10^{-3}\cos\gamma$. On the other hand, the so-called Doppler SAR imaging exploits the high Doppler-resolution wave-trains that approximate the continuous wave $e^{i\omega_0 t}$ and are characterized by large τ; in this case, the bandwidth B must be very narrow. Note that imaging using various waveforms has been thoroughly studied in [5].

Let us also note that if the cubic terms were retained when expressions (4.18) and (4.23) were substituted into the exponent in formula (4.17), we would have arrived at a similarly small degradation of the sharpness in the azimuthal direction. We would have also obtained a factor of $\mathcal{O}\left(1+\frac{v}{c}\right)$ change in the azimuthal resolution itself that could, of course, be disregarded.

5. Summary. In this paper, we have looked into whether or not the start-stop approximation used for processing radar data may affect the performance of a SAR sensor in the case of spaceborne imaging. Specifically, we have analyzed two effects that are normally left out of consideration when building the generalized ambiguity function of a radar. They are the displacement of the antenna during the pulse round-trip travel time between the orbit and the Earth's surface and the Doppler frequency shift. Our analysis shows that the displacement of the antenna, even though quite noticeable itself, in practice causes no deterioration of the image resolution. As for the Doppler effect, if the frequency shift is included in the definition of a matched filter, then the performance of the radar also remains largely unaffected. Otherwise, the imaged scene gets shifted, and there may be a small deterioration of the image sharpness.

It should also be mentioned that the authors of [5] refer to the matched filter modified by the Doppler frequency shift as a phase-corrected matched filter.

A useful future extension of the analysis presented in this paper could include taking into account the curvature of the orbit.

Appendix A. Kirchhoff integral and the Lorentz transform. The fundamental solution of the d'Alembert operator is given by

$$\mathcal{E}(t,\boldsymbol{z}) = \frac{\mathcal{H}(t)}{4\pi}\frac{\delta(|\boldsymbol{z}|-ct)}{t},$$

where $\mathcal{H}(t)$ is the Heaviside function, and $\delta(|\boldsymbol{z}|-ct)$ is a single layer of unit magnitude on the expanding sphere of radius ct centered at the origin. Then, solution of (4.2a) is given by the convolution

$$\begin{aligned}\varphi(t,\boldsymbol{z}) &= \frac{1}{4\pi}\int_0^\infty dt' \iiint_{\mathbb{R}^3} \frac{\delta(|\boldsymbol{z}-\boldsymbol{z}'|-c(t-t'))}{t-t'} P(t')\delta(z_1'-vt')\delta(z_2'-H)\delta(z_3')d\boldsymbol{z}' \\ &= \frac{1}{4\pi}\int_0^\infty \frac{\delta(|\boldsymbol{z}-\boldsymbol{x}(t')|-c(t-t'))}{t-t'}P(t')dt' \\ &= \frac{1}{4\pi}\int_{|\boldsymbol{x}|}^\infty \frac{|\boldsymbol{z}-\boldsymbol{x}(t')|\,\delta(\mu-ct)}{(c|\boldsymbol{z}-\boldsymbol{x}(t')|-(z_1-vt')v)(t-t')}P(t')d\mu \\ &= \frac{1}{4\pi}\frac{cP(t')}{c|\boldsymbol{z}-\boldsymbol{x}(t')|-(z_1-vt')v}\bigg|_{\mu=ct},\end{aligned} \tag{A.1}$$

where the new integration variable is $\mu = |\boldsymbol{z}-\boldsymbol{x}(t')|+ct' \equiv \sqrt{(z_1-vt')^2+(z_2-H)^2+z_3^2}+ct'$. To evaluate the final expression in (A.1), one needs to find the value of t' for which $\mu = ct$. This amounts to solving the equation

$$\sqrt{(z_1-vt')^2+(z_2-H)^2+z_3^2}+ct' = ct \tag{A.2}$$

with respect to t'. Equation (A.2) is a quadratic equation which is very similar to (3.8). Its solution determines the retarded moment of time when the trajectory of the moving antenna intersects with the lower portion of the characteristic cone[6] that has its vertex at $(t,\boldsymbol{z})$. The appropriate root of this equation that defines a retarded moment of time is

$$\begin{aligned}t' &= \frac{1}{\beta^2}\left(t-\frac{vz_1}{c^2}-\sqrt{\left(t-\frac{vz_1}{c^2}\right)^2-\beta^2\left(t^2-\frac{z_1^2+(z_2-H)^2+z_3^2}{c^2}\right)}\right) \\ &= \frac{\theta}{\beta}-\frac{1}{\beta c}\sqrt{\frac{(z_1-vt)^2}{\beta^2}+(z_2-H)^2+z_3^2} = \frac{\theta}{\beta}-\frac{\sqrt{\zeta_1^2+(z_2-H)^2+z_3^2}}{\beta c} = \frac{\theta}{\beta}-\frac{\rho}{\beta c},\end{aligned} \tag{A.3}$$

where we have used the definition (4.1) of the Lorentz transform. Formula (A.3) for t' is to be substituted into the numerator of the last expression in (A.1). As for the denominator of

[6] In the space $\mathbb{R}^3$, the trajectory is a horizontal straight line at altitude H; see Figure 1. However, its intersection with the characteristic cone needs to be considered in the $(3+1)$-dimensional (Minkowski) space-time, in which the trajectory becomes a straight line with the slope determined by the velocity.

this expression, using $\mu = ct$, we can write

$$\begin{aligned} c\sqrt{(z_1 - vt')^2 + (z_2 - H)^2 + z_3^2} - (z_1 - vt')v &= c^2(t - t') - (z_1 - vt')v \\ &= c^2 t - z_1 v - t'(c^2 - v^2) = c^2\left(t - \frac{z_1 v}{c^2} - t'\beta^2\right) \\ &= c^2\sqrt{\left(t - \frac{vz_1}{c^2}\right)^2 - \beta^2\left(t^2 - \frac{z_1^2 + (z_2 - H)^2 + z_3^2}{c^2}\right)} = \beta c\rho, \end{aligned} \tag{A.4}$$

where we have used formula (A.3). Altogether, substituting (A.3) and (A.4) into (A.1), we see that the expression for $\varphi(t, \boldsymbol{z})$ reduces precisely to what is given by formula (4.3), as expected.

Note that (A.2), which defines the retarded moment of time t', is so simple (quadratic) only for the case of a uniform and straightforward motion of the antenna. When the motion is accelerated and/or nonstraightforward, the resulting counterpart of (A.2) may become far more complicated; often, it can only be solved numerically as done, e.g., in [14]. In the theory of electromagnetism, the corresponding solutions of the d'Alembert equation can be interpreted as field potentials due to moving charges, and in this case they are referred to as the Liénard–Wiechert potentials; see [10, Chapter 8].

Equation (A.2) can also be solved approximately, as done, e.g., in [5]. As the square root on its left-hand side is the distance between the observation point $\boldsymbol{z} = (z_1, z_2, z_3) \in \mathbb{R}^3$ (location of the target) and the moving antenna at the moment of time t', we can represent this distance using the law of cosines and then derive an approximate expression with the help of the Taylor formula. Let γ be the angle between the velocity $\boldsymbol{v}$ and the direction from the antenna $\boldsymbol{x}(t')$ to the target $\boldsymbol{z}$; see Figure 1. Also recall that $r = \sqrt{z_1^2 + (z_2 - H)^2 + z_3^2}$. Then,

$$\begin{aligned} \sqrt{(z_1 - vt')^2 + (z_2 - H)^2 + z_3^2} &= \sqrt{r^2 + (vt')^2 - 2rvt'\cos\gamma} \\ &= r\sqrt{1 - \frac{2rvt'\cos\gamma}{r} + \left(\frac{vt'}{r}\right)^2} \\ &\approx r - vt'\cos\gamma. \end{aligned}$$

In this case, (A.2) becomes

$$r - vt'\cos\gamma + ct' = ct$$

so that its solution is

$$t' = \frac{t - \frac{r}{c}}{1 - \frac{v}{c}\cos\gamma}.$$

Substituting this expression into formula (A.1), we arrive at the solution (4.8).

Acknowledgments. The author is very thankful to Prof. Margaret Cheney for her helpful comments. It is also a pleasure to thank the anonymous referee for his or her useful suggestions.

REFERENCES

[1] O. Arikan and D. C. Munson, *A tomographic formulation of bistatic synthetic aperture radar*, in Advances in Communications and Signal Processing, Lecture Notes in Control and Inform. Sci. 129, W. A. Porter and S. C. Kak, eds., Springer-Verlag, Berlin, 1989, pp. 289–302.

[2] M. Born and E. Wolf, *Principles of Optics: Electromagnetic Theory of Propagation, Interference and Diffraction of Light*, 7th (expanded) ed., Cambridge University Press, Cambridge, UK, 1999.

[3] W. G. Carrara, R. S. Goodman, and R. M. Majewski, *Spotlight Synthetic Aperture Radar. Signal Processing Algorithms*, Artech House, Boston, 1995.

[4] M. Cheney, *A mathematical tutorial on synthetic aperture radar*, SIAM Rev., 43 (2001), pp. 301–312.

[5] M. Cheney and B. Borden, *Imaging moving targets from scattered waves*, Inverse Problems, 24 (2008), 035005.

[6] M. Cheney and C. J. Nolan, *Synthetic-aperture imaging through a dispersive layer*, Inverse Problems, 20 (2004), pp. 507–532.

[7] J. C. Curlander and R. N. McDonough, *Synthetic Aperture Radar. Systems and Signal Processing*, Wiley Series in Remote Sensing, John Wiley & Sons, New York, 1991.

[8] G. Franceschetti and R. Lanari, *Synthetic Aperture Radar Processing*, Electronic Engineering Systems Series, CRC Press, Boca Raton, FL, 1999.

[9] P. Garabedian, *Partial Differential Equations*, AMS Chelsea Publishing, Providence, RI, 2007.

[10] L. D. Landau and E. M. Lifshitz, *Course of Theoretical Physics, Vol. 2, The Classical Theory of Fields*, 4th ed., Pergamon Press, Oxford, UK, 1975.

[11] L. D. Landau and E. M. Lifshitz, *Course of Theoretical Physics, Vol. 6, Fluid Mechanics*, 2nd ed., Pergamon Press, Oxford, UK, 1987.

[12] D. C. Munson, J. D. O'Brien, and W. K. Jenkins, *A tomographic formulation of spotlight-mode synthetic aperture radar*, Proceedings of the IEEE, 71 (1983), pp. 917–925.

[13] V. S. Ryaben'kii and S. V. Tsynkov, *A Theoretical Introduction to Numerical Analysis*, Chapman & Hall/CRC, Boca Raton, FL, 2007.

[14] S. V. Tsynkov, *Artificial boundary conditions for the numerical simulation of unsteady acoustic waves*, J. Comput. Phys., 189 (2003), pp. 626–650.

[15] S. V. Tsynkov, *On SAR imaging through the Earth's ionosphere*, SIAM J. Imaging Sci., 2 (2009), pp. 140–182.